

Subsonic Boundary Layer Receptivity to Free Stream Acoustic Perturbations

Y. BANDADI¹, A. SBAIBI²

1. Faculté des Sciences et Techniques Mohammedia : gbandadi@gmail.com

2. Corresponding Author. Faculté des Sciences et Techniques Mohammedia : ahmed.sbaibi@gmail.com

Abstract

Acoustic receptivity of a Blasius boundary layer in the presence of two dimensional surface inhomogeneity is investigated numerically. It is shown that, an efficient conversion of the acoustics input to an unstable eigenmode of the boundary layer depends strongly not only on the shape but also on the width of surface roughness trough the band of Fourier Components. The location of the surface roughness is dictated by the requirement of the instability wave number at the lower branch of the stability curve derived from the Orr-Sommerfeld equations. Three different shapes are considered.

Mots clefs: *Acoustic, receptivity, Instabilities, Tollmien-Schlichting, Boundary Layer flow.*

1. Introduction

Understanding and controlling the transition from laminar to turbulent flow is necessary for optimal designs in aeronautical industries where the lower drag that characterizes the laminar flows is sought. In these situations a fuel saving up to 25% would be achieved. The process of transition in boundary layers of external flows starts from the moment an external disturbance enter the boundary layer and generates instabilities. According to (Morkovin, 1969)^[3] this process is known as Receptivity. In the case where the disturbance is an acoustic wave, energy is transferred from the acoustic wave to Tollmien-Schlichting (TS) instabilities through wavelength scattering such as in the presence of surface inhomogeneity with a finite height where the boundary layer is forced to make a rapid change in order to adjust itself. Earlier studies by (Tollmien 1929)^[9] and (Schlichting, 1933)^[8] when considering the perturbed Orr-Sommerfeld equations for a Blasius Boundary-Layer Profile show the existence of stable and unstable domain for a set of a Reynolds number based on the boundary layer thickness and a frequency parameter. These findings were confirmed by other subsequent numerical and experimental works. The boundaries between the two situations are known as the neutral curve and have a lower and an upper branch.

2. Methodology

2.1 Physical parameters of the simulation

The numerical experiment is largely inspired from the experimental work of (Saric et al. 1991)^[5] performed in wind tunnel during their study of acoustic receptivity due

to a 2-D roughness on a flat plate with a minimum leading edge effect. The roughness is located at $0.46 m$ of the leading edge which has a Reynolds number $\frac{U \delta^{\square}(x=0.46)}{\nu} = 1015$ where δ^{\square} is the BL displacement thickness, the Frequency parameter of the problem is $F = 49.33 \cdot 10^{-6}$. The acoustic wave amplitude and frequency are respectively $a = 0.01$ and $\omega = 37.354 s^{-1}$. (Figure 1) give a rough sketch of the experiment and the location of the surface roughness.

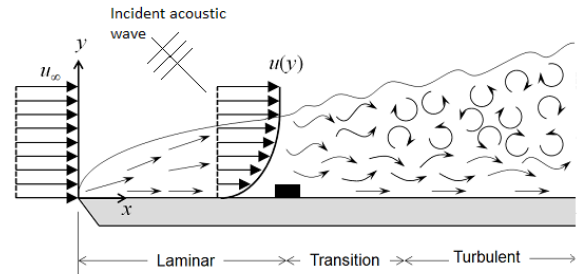


Figure 1

2.2 Conservations Equations

The conservation equations are similar to the pseudo-compressible form of the Navier-Stokes equations introduced by (Chorin, 1967)^[1]

$$\frac{\partial q}{\partial t} + \frac{\partial f}{\partial x} + \frac{\partial g}{\partial y} = \frac{1}{Re} \left[\frac{\partial (f_{\nu})}{\partial x} + \frac{\partial (g_{\nu})}{\partial y} \right]$$

The variables vector q and the inviscid flux vectors are

$$q = \begin{bmatrix} p_{\rho} \\ u \\ v \end{bmatrix} \quad f = \begin{bmatrix} \beta u \\ p_{\rho} + u^2 \\ uv \end{bmatrix} \quad g = \begin{bmatrix} \beta v \\ uv \\ p_{\rho} + v^2 \end{bmatrix}$$

$$p_{\rho} = \frac{p - p_0}{\rho_0}$$

and the viscous flux vectors are:

$$f_{\nu} = \begin{bmatrix} 0 \\ \frac{\partial u}{\partial x} \\ \frac{\partial v}{\partial x} \end{bmatrix} \quad g_{\nu} = \begin{bmatrix} 0 \\ \frac{\partial u}{\partial y} \\ \frac{\partial v}{\partial y} \end{bmatrix}$$

In the above equations Re is based on the plate length and β is a surrogate of $\rho_0 c^2$ where c is the local speed of sound.

2.3 Numerical Solution

The conservation equations are solved using a time accurate Navier Stokes code (Manno et al. 1993)^[2]. Viscous terms are approximated using central differencing while the convective terms are discretized using a third order MUSCL TVD scheme in conjunction with Riemann solver (Sbaibi et al.)^[7] Two options are used for the time advancement. An explicit, three-step, second order Runge-Kutta algorithm is used to accurately simulate the transient computations.

An implicit, approximate factorization, time advancement is used only to accelerate to steady state conditions that characterize the base flow over which a transient component is added. The computer code was extensively validated for a wide range of steady and transient flow situations including some fluid-acoustics problems (Reitsma et al. 1997)^[4].

The computer domain of (1275x52) cells includes the leading edge of the plate and an exit zone used as buffer zone. A non-uniform gridding is performed in order to capture the fine structure near the surface roughness.

The inflow boundary condition is a first order non-reflective boundary based on perturbations around the Blasius velocity profile. The boundary condition on the top sets u and v velocity gradients to zero and with the pressure calculated from the appropriate characteristic compatibility relations. A non-reflective outflow boundary condition was imposed on exit zone. Three different shape of the surface roughness were used (rectangular, cosine and exponential).

3. Results

3.1 Rectangular shape

The first numerical investigation deals with a surface roughness of rectangular shape that simulates the Mylar strip used by (Saric et al.1991)^[5] the width is set to $\lambda_{TS}/2$. A converged steady state without any acoustic source is obtained with a large CFL over 20000 time steps using the implicit approximately factored algorithm and then the calculation is restarted using an explicit Runge-Kutta method with a low CFL number. This converged steady state will provide a baseline against which to compare the unsteady solution. During the second stage of the explicit computation, the acoustic source is triggered. The acoustic wave is allowed to cross the computation domain with few wavelengths. The obtained solution is a blend of the base flow; the unsteady stokes component as well as the TS component. The Stokes solution is obtained when using the acoustic source that interacts with the boundary layer flow of a homogeneous flat plate (without roughness) as described by (Worner .2000)^[10]. A sample of the u'_{TS} at a fixed value of $y/Lref = 0.00078$ for different x location is shown in figure 2. The exponential amplification of the u'_{TS} component is clear from plot. Likewise, a plot of the u'_{TS} versus the y elevation is presented in figure 3. These two plots exhibit the same behavior and compare favorably to the largely published results. The most unstable λ_{TS} obtained from figure 2 is equal to 0.054 which is similar to the analytical value based on the linear stability theory. Plots similar to the one on figure 2 allow the calculation of the amplification

factor at different x stations downstream the surface inhomogeneity by frequency inverting method or simply by plotting $\text{Log } u'_{TS_max}$ versus x .

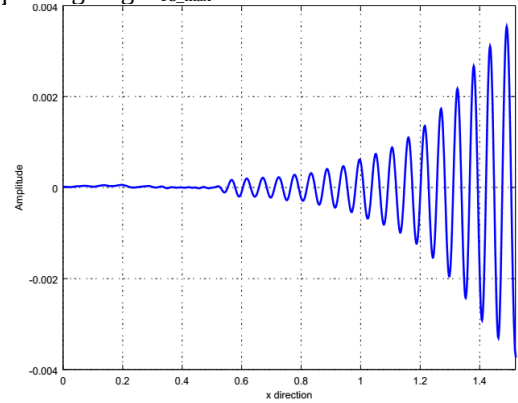


Figure 2: T-S perturbation profile of u velocity triggered by hump at $x=0.46$

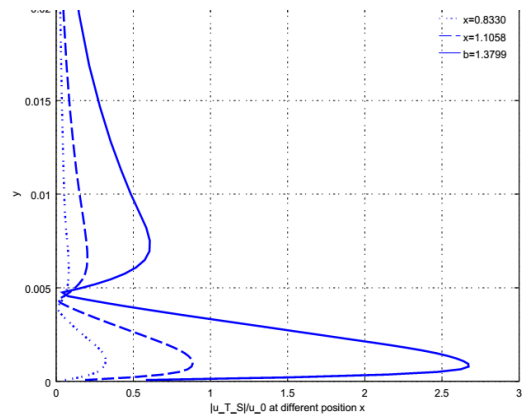


Figure 3: Amplitude of T-S waves traveling across a rectangular hump located at $x=0.46$

3.2 Effect of the roughness geometry

In this section, we present results of numerical experiments considering various shapes and different widths of the roughness. Example of u'_{TS} amplification is given on figure 4 for different shapes and a width of $\lambda_{TS}/2$. i.e $b=0.5$ where the non-dimensional number $b = \text{width} / \lambda_{TS}$. We can see that the shape does not affect the TS wavelength value but has an influence on the strength of $u'_{TS_{max}}$. However, the amplification is independent of the shape as can be seen from the slopes of $\text{Log } u'_{TS_{max}}$ in figure 4 and the subsequent figures 5 and 6. In the case of the rectangular and the exponential shapes, the higher strength is obtained with $b=0.5$ and 1.5 where area the maximum strength with the cosine shape is obtained with $b=0.5$ and 1 . For any particular shape there exists a width that does generate a weak amplitude of the $u'_{TS_{max}}$. It is corresponds to the wavelength for which the Fourier transform of the shape function vanishes. On figure 7 we plot the u'_{TS} for different shape with a width of λ_{TS} , where the receptivity of the rectangular shape vanishes. This is a clear proof of the interaction of the acoustic wave and the Fourier components.

4. Conclusion

Numerical investigation of the acoustic receptivity of a subsonic boundary layer in the presence of 2D surface inhomogeneity was conducted. The effect of the shape as

well as the effect of the width where considered. The numerical results are in very good agreement with the theoretical and other perturbation methods.^{[6][10]}

This study had put forward the superiority of the computational solver based on the advanced numerical methods inspired from the compressible CFD. The finite compressible method seems to be promising in simulating some other aero-acoustic problems that cannot be handled neither by the perturbation methods nor by incompressible CFD solvers.

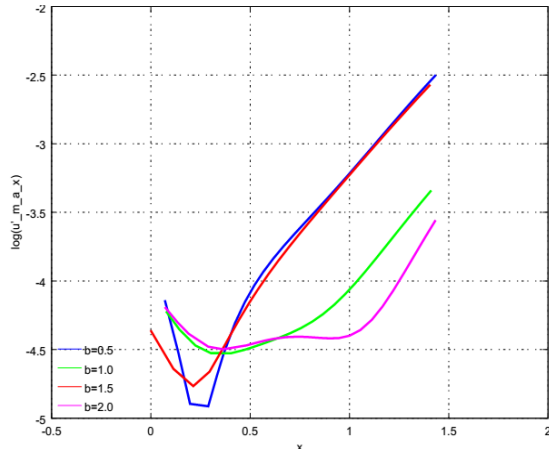


Figure 4: Amplitude growth of a T-S wave as function of width for rectangular shape

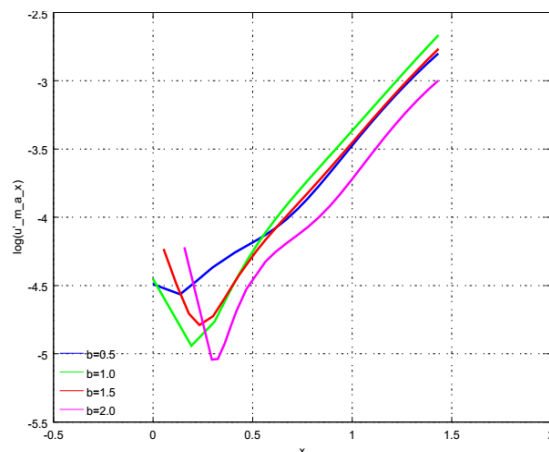


Figure 5: Amplitude growth of a T-S wave as function of width for exponential shape

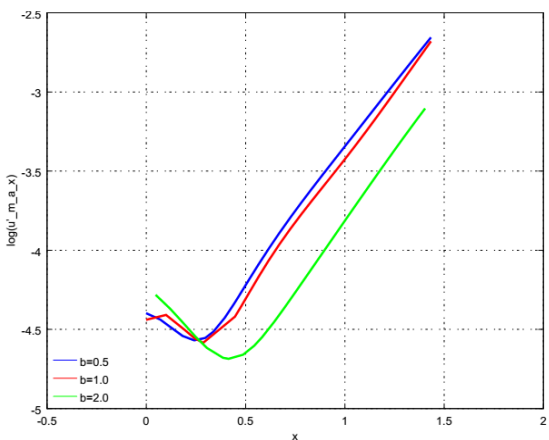


Figure 6: Amplitude growth of a T-S wave as function of width for cosin shape

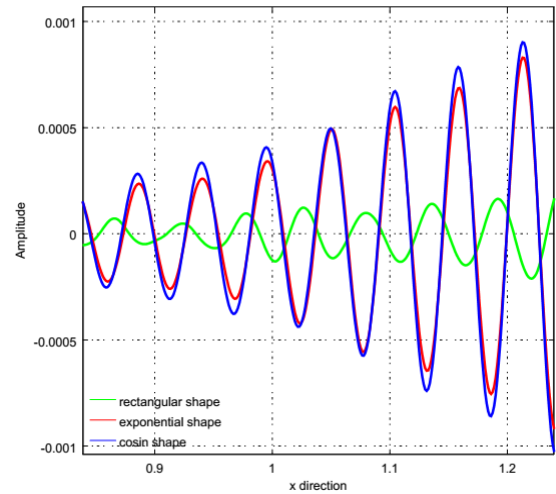


Figure 7: T-S perturbation profile of u velocity triggered by different shape at $x=0.46$

References

- [1] Chorin.A .J.1967 “A numerical method for solving incompressible Visqueuse flow problems”. *Journal of computational physics*.
- [2] Manno,V.P., Reitsma,S.H.,and Tureaud, T.F.1993."Developing Numerical Techniques for Solving Low Mach Number Fluid Acoustic Problems".*AIM Journal*,Vol.31,No.11, pp.1984-1991
- [3] Morkovin MV. 1969. “On the many faces of tran-sition. In *Viscous Drag Reduction*”, ed. CS Wells, pp. 1–31. New York: Plenum
- [4] Reitsma, S.H., Manno.V.P., and Tureaud, T.F. 1997. “Numerical Simulation of Receptivity Phenomena in Transitional Boundary-Layer Flows”, *AIAA Journal*,Vol. 35, No. 5
- [5] Saric WS, Hoos JA, Radeztsky RH Jr. 1991. “Boundary layer receptivity of sound with roughness”. See Reda et al. 1991, pp. 69–76
- [6] Tullio N “numerical evaluation of the asymptotic theory of receptivity for subsonic compressible boundary layers”.*JFM*.2015
- [7] Sbaibi.A and Manno.V.P 2000. “On the Accuracy of Upwind and Symmetric TVD Schemes in Simulating Low Mach Number Flow”.*IJCFD*. Vol. 13. pp. 125-142
- [8] Schlichting, H. 1933. “Laminar Strahlaus breitung”. *Zs. f. angew. Math. u.Mech.* Bd. 13, p. 260
- [9] Tollmien.W. 1929. “Uber die Entstehung der Turbulenz. *Nachrichten von der Gesellschaft der Wissenschaften zu Gottingen*”,Trad. NACA TM 792
- [10]Worner. A S. Herr, S. Wagner, Y.S. Kachanov , 2000. “Study of the acoustic receptivity of a blasius boundary layer in the presence of a surface non-uniformity” *European Congress on Computational Methods in Applied Sciences and Engineering*, Sep. 11-14, barcelone, Spain